ARTICLE

A Parameterization of Dry Thermals and Shallow Cumuli for Mesoscale Numerical Weather Prediction

**Julien Pergaud · Valéry Masson · Sylvie Malardel ·
Fleur Couvreux**

Abstract   For numerical weather prediction models and models resolving deep convection, shallow convective ascents are subgrid processes that are not parameterized by classical local turbulent schemes. The mass flux formulation of convective mixing is now largely accepted as an efficient approach for parameterizing the contribution of larger plumes in convective dry and cloudy boundary layers. We propose a new formulation of the EDMF scheme (for Eddy Diffusivity\Mass Flux) based on a single updraft that improves the representation of dry thermals and shallow convective clouds and conserves a correct representation of stratocumulus in mesoscale models. The definition of entrainment and detrainment in the dry part of the updraft is original, and is specified as proportional to the ratio of buoyancy to vertical velocity. In the cloudy part of the updraft, the classical buoyancy sorting approach is chosen. The main closure of the scheme is based on the mass flux near the surface, which is proportional to the sub-cloud layer convective velocity scale w_*. The link with the prognostic grid-scale cloud content and cloud cover and the projection on the non-conservative variables is processed by the cloud scheme. The validation of this new formulation using large-eddy simulations focused on showing the robustness of the scheme to represent three different boundary layer regimes. For dry convective cases, this parameterization enables a correct representation of the countergradient zone where the mass flux part represents the top entrainment (IHOP case). It can also handle the diurnal cycle of boundary-layer cumulus clouds (EUROCS\ARM) and conserve a realistic evolution of stratocumulus (EUROCS\FIRE).

Keywords   Atmospheric boundary layer · Detrainment · Entrainment · Mass flux ·
Parameterization · Shallow convection · Turbulence

J. Pergaud (✉) · V. Masson · S. Malardel · F. Couvreux
CNRM - GAME, Groupe de Modélisation à Moyenne Échelle,
Météo-France, 42 Avenue Gaspard Coriolis, BP 31077 Toulouse, France
e-mail: julien.pergaud@numtech.fr

⌷ Springer

1 Introduction

The parameterization of shallow convection and more generally the mixing in the boundary layer is an important issue in atmospheric numerical models. Moreover, shallow clouds play an important role in the energy budget of the atmosphere through their impact on the incoming shortwave radiation. At the 2-km resolution, typical of current numerical weather prediction (NWP) models, deep convection is resolved but dry and cloudy shallow convection and turbulence must still be parameterized. Therefore, improving the representation of physical processes (turbulent local transport, thermals and shallow clouds) in the planetary boundary layer (PBL) is still an important issue in NWP. In particular, the representation of subgrid vertical fluxes, cloud fraction and cloud water needs to be improved (Teixeira et al. 2008).

In a dry or cloudy convective boundary layer (CBL), the evolution of a variable ϕ is strongly influenced by vertical turbulent transport. Therefore, a good estimation of the second-order moment $\overline{w'\phi'}$ is needed to determine the trend of $\overline{\phi}$ correctly.

Eddy diffusivity or K-theory was the first approach used to parameterize the vertical mixing in the PBL, where the turbulent flux is expressed as a function of the vertical gradient of the mean variable. Nevertheless, this formulation fails to represent the upper part of a dry CBL where the turbulent heat transport is opposed to the mean potential temperature ($\overline{\theta}$) gradient (Deardorff 1966; Schumann 1987). A solution was developed to represent the non-local effect of the large eddies by adding a countergradient term to the K-theory (Deardorff 1966; Holtslag and Moeng 1991; Cuijpers and Holtslag 1998; Tomas and Masson 2006). Another historical approach is "mass flux" parameterization, first introduced in studies of cumulus convection (Ooyama 1971; Betts 1973; Yanai et al. 1973; Arakawa and Schubert 1974; Tiedtke 1989; Bechtold et al. 2001). This formulation describes the vertical ascent of convective structures, where a top-hat distribution is used to divide the grid cell into an updraft zone and its surrounding environment (Arakawa and Schubert 1974).

Siebesma and Teixeira (2000) and Hourdin et al. (2002) have developed a new parameterization that combines eddy-diffusivity and mass flux approaches in a consistent way. Organized strong updrafts are parameterized by the mass flux part while the remaining turbulence is parameterized using K-theory. This parameterization, named EDMF (Eddy Diffusivity\Mass Flux), was developed to model cloudy shallow convection and dry convection in a unified way. In the EDMF framework, the turbulent flux of a conservative variable ϕ is defined as:

$$\overline{w'\phi'} = -K\frac{\partial\overline{\phi}}{\partial z} + \frac{M_u}{\rho}(\phi_u - \overline{\phi}), \tag{1}$$

where ρ is the density, K is the turbulent diffusivity, M_u is the convective mass flux $M_u = \rho a_u w_u$ (a_u is the updraft fraction area and w_u is the vertical velocity in the updraft), $\overline{\phi}$ is the mean value and ϕ_u is the updraft value of the variable ϕ.

In this formulation, it is assumed that the size of the updraft area is very small compared to the grid size ($a_u \ll 1$), so the environmental values are considered equal to the mean values. The effect of downdrafts is neglected as this parameterization is used only for shallow convection. Siebesma and Cuijpers (1995) and Wang and Stevens (2000) have shown that the mass flux contribution in Eq. 1 can represent 80–90% of the total flux of conservative variables (conservative without precipitation): the liquid potential temperature (θ_l) and the total mixing ratio (r_t). The eddy-diffusivity term represents the remaining fluctuations due to non-organized local turbulence. The EDMF concept is well suited to modelling boundary-layer physical processes leading to shallow convection and shallow cloud formation.

Table 1 Main characteristics of the previous EDMF schemes

	SMST04	SST07	RH08
Dry portion equations	w_u	w_u	w_u, M_u
Cloudy portion equations	w_u, M_u		w_u, M_u
Closure	LCL:a_c	Grd:σ_w	Grd: $w_u = 0, a_u$
	Grd:w_u		z_s: $M_u = \sum_k E_s(k)$
Updraft fractional area	Constant		a_u Profile
Cloud fractional area	Variable		
Dry entrainment	$\epsilon = c_\epsilon \left(\frac{1}{z} + \frac{1}{z_i - z} \right)$	$\epsilon = c_\epsilon \left(\frac{1}{z} + \frac{1}{z_i - z} \right)$	$E(z) = E_s(z) + \beta D(z)$
Dry detrainment			$D(z) = \frac{\partial}{\partial z} \left(\frac{\rho w_u \sqrt{\lambda z}}{r z_t} \right)$
Cloudy entrainment	Constant		Constant
Cloudy detrainment	Constant		Constant
Momentum transport			ED\MF

SMST04 stands for Soares et al. (2004), SST07 for Siebesma et al. (2007) and RH08 for Rio and Hourdin (2008). Crucial points are definitions of entrainment and detrainment and the closure of the scheme. Grd is for ground and LCL for lifting condensation level

The main purpose of our article is to present a new set of parameterizations based on the EDMF concept. The EDMF approach has been implemented in various versions: a first version was implemented by Soares et al. (2004) (SMST04) in the research model Meso-NH some years ago. Meanwhile, other parameterizations based on the same concept have been developed (SST07 for Siebesma et al. (2007) and RH08 for Rio and Hourdin (2008)). Their characteristics are summarized in Table 1. First, in the dry portion of the CBL, Soares et al. (2004) and Siebesma et al. (2007) diagnosed the mass flux from the vertical velocity w_u. Assuming a constant updraft fraction, they only needed a definition for the dry entrainment, and used an empirical definition for entrainment based on De Roode et al. (2000). Hourdin et al. (2002) diagnosed the mass flux at the top of the surface layer (z_s) as the sum of the entrainment in this layer. Above, entrainment vanishes and only the detrainment is defined to obtain a given profile of the updraft fractional area (a_u). Rio and Hourdin (2008) modified this entrainment (Table 1). More explanations are to be found in these references.

In the cloud layer, entrainment and detrainment have always been considered constant in these parameterizations, as in Tiedtke (1989). These quantities have been defined by Siebesma and Holtslag (1996) from large-eddy simulations (LES) of a trade-wind cumulus case although other complex formulations have been used in mass flux parameterizations. Moreover, Soares et al. (2004) used the mass flux equation in the cloudy portion and closed the scheme using a constant cloud fractional area at the lifting condensation level (LCL).

The main motivations for developing a new version using the EDMF concept were:

– to improve the representation of cloud characteristics: liquid water content and cloud fraction;
– to improve the mixing in the CBL, notably in the countergradient transport where eddy diffusivity is insufficient (Stull 1988);
– to retain the Kain and Fritsch (1990) approach and so enable vertical variations of entrainment and detrainment in the cloudy portion;
– to have adaptive dry entrainment and detrainment depending on the type of the CBL and the strength of convection, and limit the impact of the scheme if conditions are unfavourable for convection development;

- to enable variations of updraft area fraction, which is taken as constant in several previous formulations;
- to improve the mixing of momentum.

In Sect. 2, we describe the updraft model and the definition of entrainment and detrainment in dry thermals and also within clouds for shallow cumulus cases. The subgrid cloud scheme is also introduced. In Sect. 3, the scheme is evaluated via comparisons with LES on different case studies.

2 Description of the Convection Scheme

2.1 Updraft Model

The updraft model is defined as a single entraining/detraining rising parcel as in Soares et al. (2004). One resulting updraft described by the mass flux is used to represent the effect of several plumes, and its characteristics are determined as a function of mixing between the updraft and its environment through entrainment E (the inward mass flux from the environment to the updraft) and detrainment D (the outward mass flux). Moreover, in the mass flux approximation, the cloud ensemble is considered in the steady state. The mass flux is defined as $M_u = \rho a_u w_u$, and its evolution is determined by a diagnostic equation of the mass continuity between the updraft and its surrounding environment (Fig. 1),

$$\frac{\partial M_u}{\partial z} = (E - D) \tag{2}$$

or,

$$\frac{1}{M_u}\frac{\partial M_u}{\partial z} = (\epsilon - \delta) \tag{3}$$

where ϵ and δ are respectively the entrainment rate ($E = \epsilon M_u$) and the detrainment rate ($D = \delta M_u$).

The evolution of a conserved parcel characteristic ϕ_u during the ascent is defined as in Siebesma (1998):

$$\frac{\partial M_u \phi_u}{\partial z} = E\overline{\phi} - D\phi_u \tag{4}$$

using Eq. 2 and simplified as:

$$\frac{\partial \phi_u}{\partial z} = -\epsilon(\phi_u - \overline{\phi}) \tag{5}$$

where ϕ_u and $\overline{\phi}$ are respectively an updraft conserved variable and its mean value on the grid. This equation is used to determine the evolution of updraft conservative variables such as the liquid potential temperature θ_{lu} and the total mixing ratio r_{tu} during ascent.

The vertical velocity (w_u) equation for the updraft is given by:

$$w_u \frac{\partial w_u}{\partial z} = B_u - \epsilon w_u^2 - P \tag{6}$$

where on the right-hand side (rhs), the first term is the buoyancy, the second term is the entrainment, and P represents the pressure term defined, e.g. in Simpson and Wiggert (1969),

Fig. 1 Variations of the updraft characteristics M_u, θ_{lu} and r_{tu} dependent on the mixing with the environment dictated by the entrainment ϵM_u and the detrainment δM_u
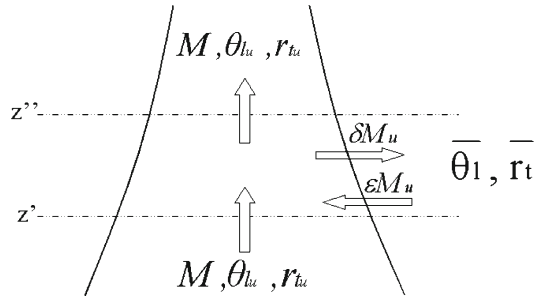
Siebesma et al. (2003), Soares et al. (2004) as a linear combination of the first two terms. Therefore, the equation can be simplified as:

$$w_u \frac{\partial w_u}{\partial z} = a B_u - b\epsilon w_u^2 \tag{7}$$

where $a = 1$ and $b = 1$, defined respectively as a virtual mass coefficient and a drag coefficient (Simpson and Wiggert 1969). Numerical aspects are given in Appendix 2.

Using the definition of mass flux, Soares et al. (2004) and Siebesma et al. (2007) computed the mass flux in the dry portion of their updraft directly from the vertical velocity obtained from Eq. 7 and using a constant fractional area. At the cloud base, they used a constant value of the cloud fractional area to compute the mass flux and close the scheme.

Here, Eq. 7 is used to define the top of the updraft where w_u vanishes and also to diagnose the updraft fraction area, a_u, which is not a constant or a closure of the scheme as in Soares et al. (2004) and Siebesma et al. (2007).

Here, thanks to the independent computations of both mass flux M_u (Eq. 3) and w_u (Eq. 7), the updraft fraction area can vary vertically, and is defined as

$$a_u = \frac{M_u}{\rho w_u}. \tag{8}$$

The vertical variations of this last variable are important because a_u is used to diagnose the cloud fraction (see next section).

Only Hourdin et al. (2002) and Rio and Hourdin (2008) apply their scheme to momentum mixing, processing the wind component as a conservative variable. Here, the mass flux approach is used to perform a non-local mixing of momentum along the vertical in addition to the mixing already performed by the turbulent scheme via the eddy-diffusivity approach. But, since the momentum is not conservative, the effect of pressure perturbations is added using a parameterization from Gregory et al. (1997). The evolution of the updraft horizontal wind component is defined as:

$$\frac{\partial u_u}{\partial z} = -\epsilon(u_u - \overline{u}) + C_u \frac{\partial \overline{u}}{\partial z}, \tag{9}$$

$$\frac{\partial v_u}{\partial z} = -\epsilon(v_u - \overline{v}) + C_v \frac{\partial \overline{v}}{\partial z}, \tag{10}$$

where $C_u = C_v = 0.5$, and u_u (v_u) represents the zonal (meridional) component of wind speed modified during the ascent in the updraft; $\overline{u}$ and $\overline{v}$ are zonal and meridional mean wind components respectively.

2.2 Lateral Mass Exchanges

The definition of entrainment and detrainment is the crucial issue in this type of parameterization. Various studies have used different definitions for various PBL regimes (e.g. Siebesma, 1998; Neggers et al., 2002; De Rooy and Siebesma, 2008). Using LES results, De Roode et al. (2000) showed that, for the dry CBL, the entrainment rate could be approximated by:

$$\epsilon = cz^{-\alpha} \tag{11}$$

with α close to 1. This formulation takes the entrainment dependence on height into account. Siebesma and Teixeira (2000) used another formulation to define lateral exchanges in the dry portion of the CBL: $\epsilon = 1/z + 1/(z_i - z)$ where z_i is the inversion height. In this formulation applied by Soares et al. (2004), ϵ is only dependent on geometrical aspects but independent of the type of boundary layer or the intensity of the thermals in convective regime. Rio and Hourdin (2008) defined the detrainment rate from other geometrical considerations, where detrainment is regulated to reduce the width of the thermal from the surface to z_i, becoming zero at the top of the CBL. Moreover, the entrainment rate is defined as proportional to the detrainment rate in the dry portion of the CBL.

Here, we have chosen to define lateral mass exchanges from physical characteristics of the CBL. Arakawa (2004) explains that buoyancy is an important parameter in shallow convection. Moreover, the vertical velocity w_u is considered as a pertinent parameter in the description of mixing between dry updraft or the cloud and their environment in shallow convection. Neggers et al. (2002) define the entrainment as inversely proportional to vertical velocity for shallow cumulus convection, and Cheinet (2003) also applies this formulation to dry plumes. This means that ϵ is not constant but decreases with higher vertical velocities. In other words, an updraft with strong vertical velocity will be isolated from its environment.

Here, in the dry portion of the CBL, ϵ and δ are no longer dependent on z (Eq. 11) but take physical characteristics of a buoyant ascending parcel into account. Equation 7 shows that buoyancy is linked to vertical velocity, $w_u{}^2$ being a vertical integral of the buoyancy. However, locally, both can be independent, for example in the non-buoyant part where negative buoyant air can still be ascending. Young (1988) explains that the correlation between the buoyancy and w decreases in the upper part of the CBL, the buoyancy acting as a displacing force in the lower part of the CBL and as a restoring force in the upper part of the CBL. Thus, lateral mixing does not only depend on vertical velocity as in Neggers et al. (2002) but must be locally defined as an equilibrium between w_u and buoyancy B_u. By dimensional analysis (Buckingham 1914), we obtain:

$$\epsilon_{dry}, \delta_{dry} \propto \frac{B_u}{w_u^2} \tag{12}$$

where $B_u = g(\theta_{v,u} - \overline{\theta_v})/\overline{\theta_v}$ is the buoyancy.

Near the ground, relatively strong buoyancy and weak vertical velocity allow strong entrainment to import many air parcels into the updraft, implying a positive proportionality coefficient for ϵ. Near the inversion, in the non-buoyant zone, much air is detrained implying a negative proportionality coefficient for δ. Since entrainment and detrainment rates cannot be negative, the entrainment rate is zero where the updraft is non-buoyant compared to its surrounding environment. Conditional sampling of detrainment in LES has shown that detrainment is not null in the mixed layer (Fig. 9c), so to keep a positive detrainment in the buoyant part of the updraft, a minimum detrainment is defined using a modified formulation from Lappen and Randall (2001): $\delta = (L_{up} - z)^{-1}$.

Eventually, in the dry portion of the CBL, entrainment and detrainment are defined as:

$$\epsilon_{dry} = Max\left[0, C_\epsilon \frac{B_u}{w_u^2}\right], \tag{13}$$

$$\delta_{dry} = Max\left[\frac{1}{L_{up} - z}, C_\delta \frac{B_u}{w_u^2}\right], \tag{14}$$

where L_{up} is the Bougeault and Lacarrère (1989) (BL89) upward mixing length, C_δ and C_ϵ have been tuned to fit one-dimensional (1D) entrainment and detrainment to LES, $C_\delta = -10$ and $C_\epsilon = 0.55$. Numerical aspects are given in Appendix 3.

There are several descriptions of the exchanges in the cloudy portion. Simpson and Wiggert (1969) defined entrainment and detrainment rates as functions of the cloud radii. In the parameterizations of Tiedtke (1989), the entrainment and detrainment rates are constant $\epsilon = \delta = 2 \times 10^{-4}$ m^{-1}. Using LES results, Siebesma and Cuijpers (1995) showed that typical entrainment and detrainment values are one order of magnitude higher than the values used in Tiedtke (1989) and that the detrainment rate is larger than the entrainment rate, thus allowing a decreasing mass flux in the cloud. They found typical values for ϵ and δ of 2×10^{-3} and 3×10^{-3} m^{-1} respectively. Soares et al. (2004) and Rio and Hourdin (2008) also used these fixed values for entrainment and detrainment (Table 1).

We chose to define two different types of exchange differentiating the dry portion of the updraft from the moist one because the environment of any updraft is strongly turbulent compared to the environment of a cloud. Taylor and Baker (1991) have emphasised the importance of buoyancy sorting in determining the cloud composition and in defining a continued lateral entrainment and detrainment. Zhao and Austin (2003) explained that a buoyancy sorting model could be used as a physically more realistic alternative to entraining plume models in shallow cumulus convection notably resolving the Warner paradox. In the parameterization presented here, if the lifting condensation level (LCL) is reached, lateral exchanges are computed using the parcel buoyancy sorting approach of Kain and Fritsch (1990) (KF90 in the following). Details are given in Kain and Fritsch (1990) and Bechtold et al. (2001).

2.3 Scheme Initialization and Closure

Usually, convection schemes use a closure at the lifting condensation level (LCL), and Neggers et al. (2004) studied the impact of different types of closure at the cloud base. They showed that the closure developed by Grant (2001) for shallow cumulus using the subcloud convective velocity scale w_* (Deardorff 1980b) gave satisfactory results due to the fact that the subcloud turbulence drives the transport at cloud base. Our approach is consistent with these results. Real dynamical continuity links the subcloud layer to the cloud layer, so M_u at LCL is computed directly from the mass flux equation (Eq. 2), and takes the mixing processes into account for the whole subcloud layer.

Since the scheme starts from the surface, $M_u(z_{grd})$ is computed as a function of w_* but at the surface, unlike the closure at the cloud base defined by Grant (2001),

$$M_u(z_{grd}) = C_{M0}\rho \left(\frac{g}{\theta_{vref}} \overline{w'\theta'_{vs}} L_{up}\right)^{1/3} \tag{15}$$

where $\overline{w'\theta'_{vs}}$ is the surface buoyancy flux, L_{up} is the BL89 upward mixing length corresponding to the distance that a parcel leaving the ground travels due to buoyancy. The value

of $C_{M_0} = 0.065$ is based on LES results and its determination is given in Appendix 1. Note that, in the surface layer, this value is greater than the value $C_{M_0} = 0.03$ originally proposed by Grant (2001) at the LCL.

The rising parcel characteristics are determined at the ground using the formulation of Soares et al. (2004) in which an excess is added to the environmental values. For example, the updraft liquid potential temperature near the ground is:

$$\theta_{lu}(z_{grd}) = \overline{\theta_l}(z_{grd}) + \alpha \frac{\overline{w'\theta'_l}_s}{e^{1/2}(z_{grd})} \tag{16}$$

where the value of α is 0.3 as in Soares et al. (2004). Sensitivity tests indicate (in the range [0, 1]) that results are not dependent on this coefficient (not shown). This excess is formulated as a function of the surface-layer variability according to Troen and Mahrt (1986) who demonstrated that the excess is well correlated with the ratio of the surface heat flux and the square root of turbulent kinetic energy. A similar equation is used for r_t.

At the surface, w_u is initialized from the turbulent kinetic energy e (provided by the turbulence scheme),

$$w_u^2(z_{grd}) = \frac{2}{3} e(z_{grd}). \tag{17}$$

2.4 The Subgrid Condensation Scheme

The updraft scheme must represent the evolution of an air parcel during its ascent including not only dynamical but also thermal evolutions, noting that the parcel can condense. Therefore, a subgrid cloud is diagnosed from the updraft characteristics. Although conservative variables are used, we diagnose a subgrid liquid mixing ratio $r_{c_{up}}$ and a cloud fraction CF; $r_{c_{up}}$ is computed from θ_l, r_t and pressure using a "all or nothing" variation scheme since the updraft air parcels are considered to be completely cloudy. CF is defined as proportional to the updraft fraction on the grid a_u:

$$CF = C_{cf} a_u \tag{18}$$

where $C_{cf} = 2.5$. The horizontal size of the cloud is taken as 2.5 times greater than the size of the updraft; this parameter was tuned to fit the 1D cloud fraction to LES results. The coefficient represents the difference between the cloudy core fraction and the cloud fraction.

The liquid mixing ratio is approximated as the product of the previously computed cloud fraction and the updraft liquid mixing ratio computed from the updraft conservative variables (Bechtold and Cuijpers 1995):

$$\overline{r_c} = r_{c_{up}} CF. \tag{19}$$

In our parameterization, r_c is not a prognostic variable. If the mass flux becomes zero, the cloud disappears totally. Only a prognostic cloud scheme can lead to evaporation of a cloud over several timesteps. So, passive clouds that are not maintained by a thermal are not taken into account in the parameterization. However, here, $\overline{r_c}$ represents only the contribution of the shallow convection clouds. Other contributions for clouds can arise from the subgrid turbulence scheme or from the microphysical scheme (notably for resolved clouds).

3 Evaluation of 1D Results with Large-Eddy Simulations

3.1 The Numerical Model

The model used to simulate these different convection cases is the non-hydrostatic model Meso-NH (Lafore et al. 1998), which can be used in various configurations: mesoscale meteorological model, cloud resolving model (CRM) or LES. The turbulence scheme is the 1.5-order prognostic turbulence scheme developed by Cuxart et al. (2000), which is activated for all single column model (SCM) simulations and enables the computation of the eddy-diffusivity component of the turbulent fluxes (Eq. 1). In LES simulations, the turbulence scheme is three-dimensional while it is purely vertical (and coupled to the mass flux scheme) in the 1D simulations. For each of the meteorological situations simulated below, two simulations were run:

– an LES simulation considered as the reference;
– a 1D simulation with mass flux included.

In addition, in order to highlight the transport linked to the thermals in a dry CBL and stratocumulus PBL, another 1D simulation was performed without the mass flux scheme (only the turbulence scheme was activated).

Note, too, that although no observations were used for validation, we followed the Global Energy and Water Cycle Experiment Cloud System Study (GCSS) methodology (Browning 1993) consisting of using observations to evaluate the LES that is then used to validate SCM results. Finally, Siebesma et al. (2003) and Brown et al. (2002) have shown that LES are robust for representing shallow cumulus convection and Duynkerke et al. (2004) have shown that this is also the case for a stratocumulus-topped boundary layer.

3.2 Dry Convective Boundary Layer

The first case tested with the new parameterization is a case from a dataset collected during the International H_2O project (IHOP) described by Weckwerth et al. (2004). This field experiment took place in the US Southern Great Plains (SGP) from 13 May to 25 June 2002. Here, we use the 14 June 2002 day corresponding to a growing CBL near Homestead, Oklahoma. The LES was evaluated against soundings, aircraft and lidar measurements (Couvreux et al. 2005). Initial profiles for potential temperature and water vapour mixing ratio and prescribed surface fluxes were used in LES and SCM (Fig. 2). The same vertical resolution was applied (58 levels, resolution better than 100 m below 2,500 m and up to 150 m higher up) in the LES and SCM. The timestep was fixed at 60 s. Forcing to take account of mesoscale advection was added as in Couvreux et al. (2005). The configurations of these simulations are summarized in Table 2.

Figure 2 shows θ_l and r_t profiles after 3 and 6 h of simulation for LES, SCM simulation with the new scheme and SCM simulation using only the turbulence scheme. A significant improvement of the dry CBL representation was achieved by adding the mass flux term. With the turbulence scheme only, the model fails to represent the countergradient zone. When only the eddy-diffusivity term is taken into account in Eq. 1, no turbulent transport opposed to the gradient is represented. Without mass flux, the top entrainment is incorrectly represented leading to a too-low inversion and a too-cold and too-moist CBL.

Adding the mass flux contribution to the turbulent fluxes enables the development of the CBL to be accurately simulated. The inversion is well located according to LES and the countergradient zone is well simulated.
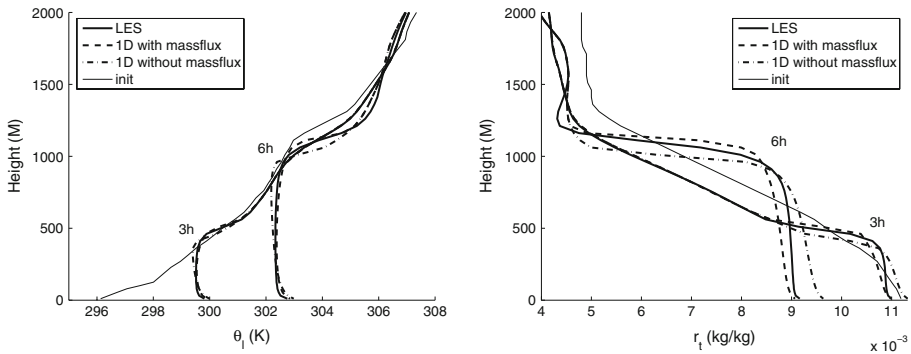
Fig. 2 IHOP case: Vertical profiles of liquid potential temperature θ_l and total mixing ratio r_t after 3 and 6 h of simulation. *Solid thin line* is the initial profile, *solid line* represents LES results, *dashed line* the SCM simulation with the new parameterization and *dashed-dotted line* the profile obtained using only the turbulence scheme

Table 2 Configurations of the different simulations for the different cases studied including vertical grid size at the inversion and in the mixed layer, horizontal resolution only for LES and timestep

	IHOP	ARM	FIRE
Configuration	LES/SCM	LES/SCM	LES/SCM
Δx, Δy (LES) (m)	100	100	50
Δz Mixed layer (m)	20–50	40	10
Δz Inv. (m)	50	40	10
Δt (SCM) (s)	60	60	60

The turbulent fluxes obtained from the SCM are very similar to the LES turbulent fluxes (Fig. 3). The gradient of these fluxes are comparable leading to a correct estimation of the evolution of conservative variables. The eddy diffusivity mainly contributes to the turbulent fluxes in the lower part of the BL while the mass flux contribution predominates in the upper part. Local mixing due to small eddies is important near the ground whereas the non-local mixing, due to the large eddies, has an impact in the upper part of the CBL. The fact that the mass flux part is the only contribution to the mixing near the inversion can be explained by the overshooting of updrafts responsible for top entrainment enabling the CBL growth. This agrees with the study of Sullivan et al. (1998) who showed, using LES, that overshooting thermals are responsible for top entrainment in a dry CBL.

Figure 4 shows that the new parameterization improves the wind profiles throughout the simulation, and adding a non-local transport contribution improves the variability of the momentum fluxes.

To conclude, these different results show the capability of the scheme in representing the development of a growing CBL from a stable nocturnal layer. The new scheme was also tested on another case of dry convection from a dataset collected during the Wangara Experiment (Clarke et al. 1971). Similar results were found.

3.3 Diurnal Cycle of Cumulus Over Land: EUROCS\ARM

The EUROCS\ARM case study is a well-documented typical case of shallow convection, and is based on an idealisation of the experiment performed at the Southern Great Plains
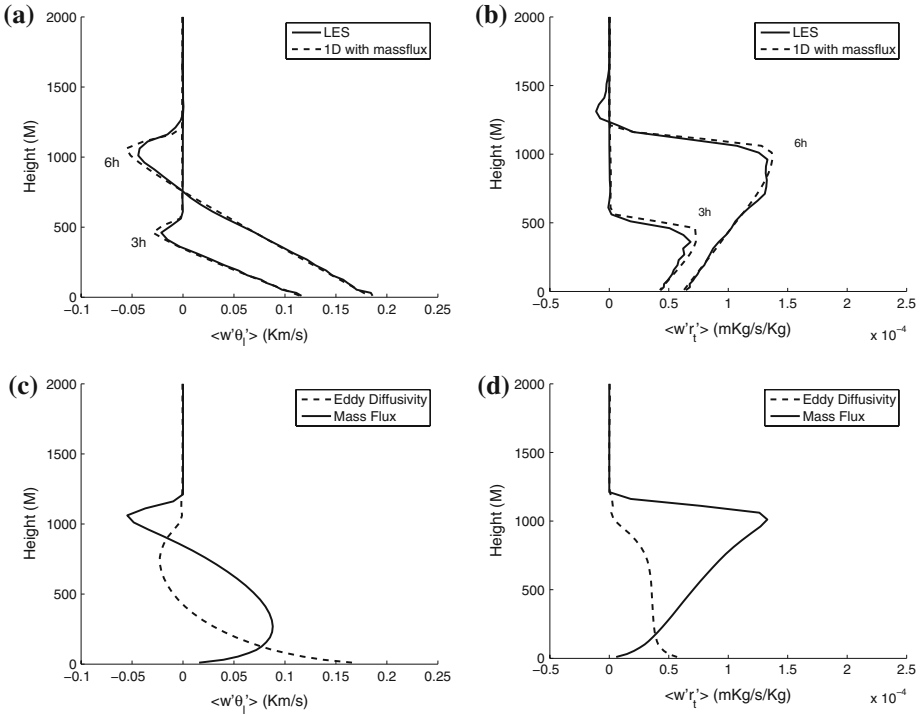
Fig. 3 IHOP case: Turbulent fluxes **a** $\overline{w'\theta'_l}$ and **b** $\overline{w'r'_t}$ after 3 and 6 h of simulation. *Solid line* represents LES results, *dashed line* SCM results with the new parameterization. Contributions of the eddy-diffusivity term (*dashed line*) and mass flux term (*solid line*) in the computation of **c** $\overline{w'\theta'_l}$ and **d** $\overline{w'r'_t}$
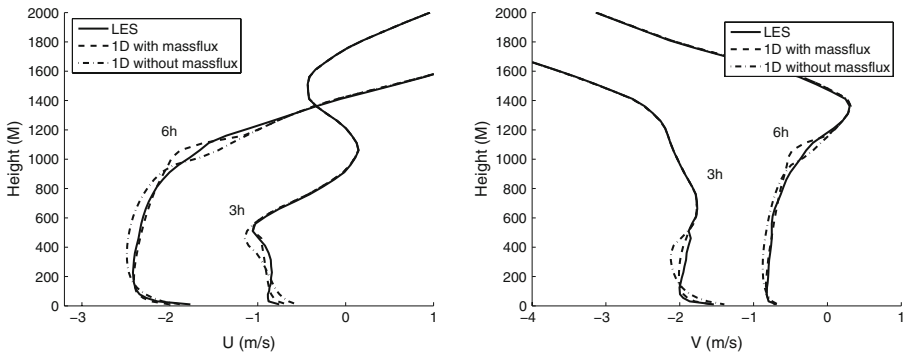

Fig. 4 IHOP case: *U* and *V* profiles after 3 and 6 h of simulation. *Solid line* represents LES results, *dashed line* SCM results with the new parameterization and *dashed-dotted line* the profile obtained using only the turbulence scheme

site of the Atmospheric Radiation Measurement (ARM) Program during the European cloud systems project (EUROCS). Brown et al. (2002) presented this case of a diurnal cycle of cloudy convection over land. The objective here was to simulate the development of a CBL over land, where forcing is generally both stronger and varies more with time varying than

over the ocean. SCM simulations were performed using the same vertical stretched grid as used in LES: 100 levels were used with constant vertical resolution of 40 m up to 4,000 m as in Brown et al. (2002). The timestep was set to 60 s. Initial profile, prescribed surface fluxes and forcing were the same than those discussed by Brown et al. (2002) and used for LES. The configurations of these simulations are summarized in Table 2.

3.3.1 Conservative Variables and Turbulent Fluxes

Figure 5 shows θ_l and r_t profiles at different times. The results obtained with the SCM are very consistent with those obtained by LES, and CBL growth is well-represented by the model with the new parameterization: the inversion is well-positioned. The model represents the evolution of $\overline{\theta}_l$ and $\overline{r}_t$ consistently in both the dry and the cloudy portions.

Figure 6 shows mean profiles of turbulent fluxes averaged over 8–9h. The SCM results of turbulent fluxes are consistent with those obtained from LES in the dry portion of the CBL. But in the cloud layer (between 1,100 and 2,000 m), turbulent fluxes are slightly weaker than in LES. Note that there is no discontinuity at the lifting condensation level (LCL) where the computation of entrainment and detrainment changes.
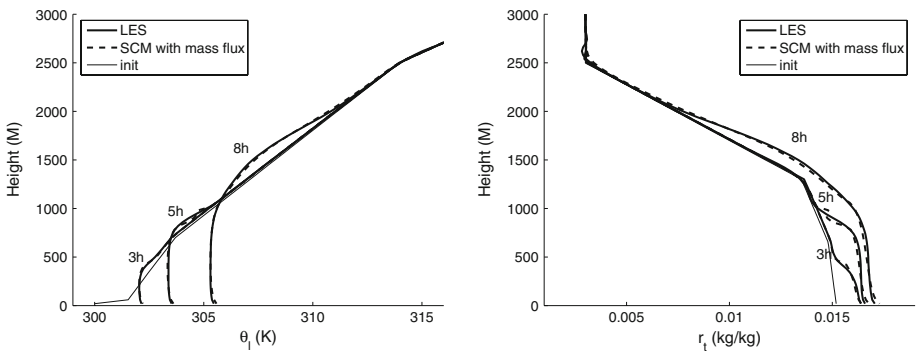

Fig. 5 ARM case: θ_l and r_t profiles after 3, 5, 8 h of simulation. *Solid thin line* is the initial profile, *solid line* for LES results, *dashed line* for results with the new parameterization
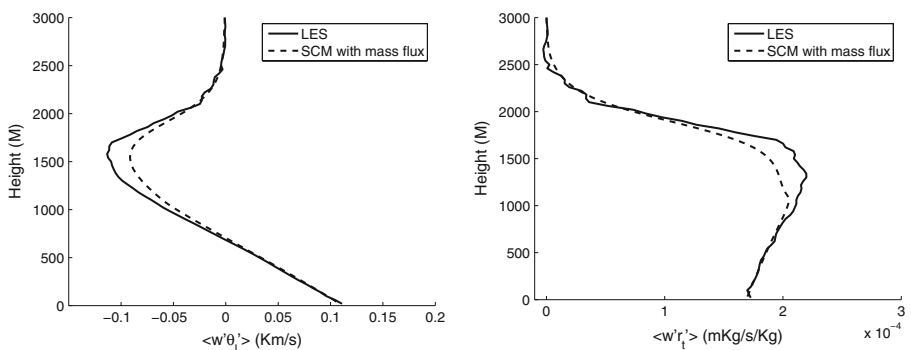

Fig. 6 ARM case: turbulent fluxes $\overline{w'\theta'_l}$ and $\overline{w'r'_t}$ profiles averaged over 8–9 h. *Solid line* represents LES and the *dashed line* SCM with the new parameterization

3.3.2 Cloud Variables

Lenderink et al. (2004) have shown in their SCM intercomparison study that SCMs have a number of general deficiencies: "too large values of cloud cover and cloud liquid water, unrealistic thermodynamic profiles and high amounts of numerical noise". In recent studies, dealing with shallow cumulus parameterization, the liquid water mixing ratio r_c and the cloud fraction are still misdiagnosed by SCMs. For example, in Soares et al. (2004), $\overline{r_c}$ is overestimated or underestimated due to a lack of mixing of the conservative variables and the cloud fraction is too large.

With the new set of parameterizations proposed here, there is no numerical noise and thermodynamic profiles are consistent with those obtained using LES (as shown previously). The cloud fraction and the cloud liquid water $\overline{r_c}$ are well-modelled by the subgrid condensation scheme, as illustrated in Fig. 7 showing the profile of the liquid mixing ratio and the cloud fraction averaged over 8–9 h. Qualitatively, 1D values of $\overline{r_c}$ and cloud fraction are similar to LES results, notably the decrease of this variable with height.

The cloud-base and cloud-top evolutions are shown in Fig. 8; the cloud formation and dissipation are well-modelled in terms of time as well as height.
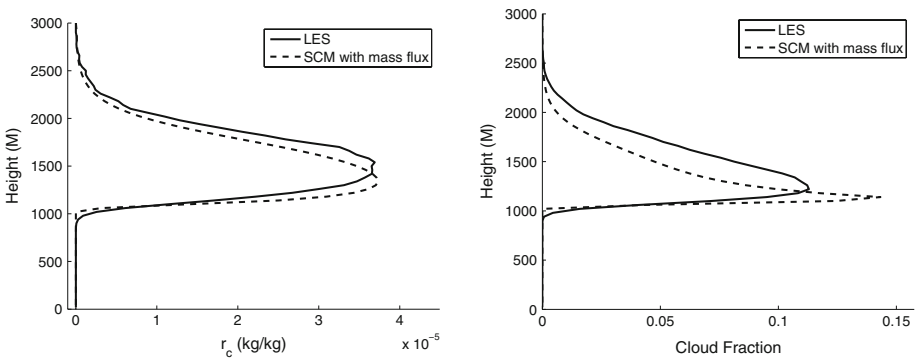

Fig. 7 ARM case: liquid mixing ratio r_c profile and cloud fraction profiles averaged over 8–9 h. *Solid line* shows LES results, *dashed line* 1D results with the new parameterization
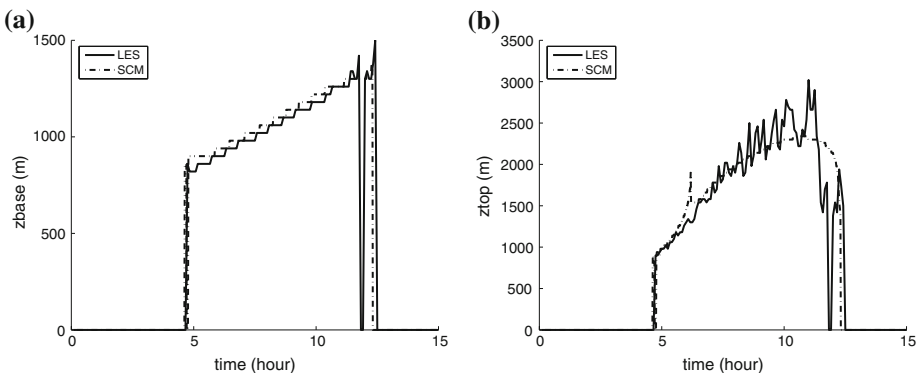

Fig. 8 ARM case: evolution of the cloud base (**a**) and cloud top (**b**). *Solid line* shows LES results and *dashed dotted line* is for SCM
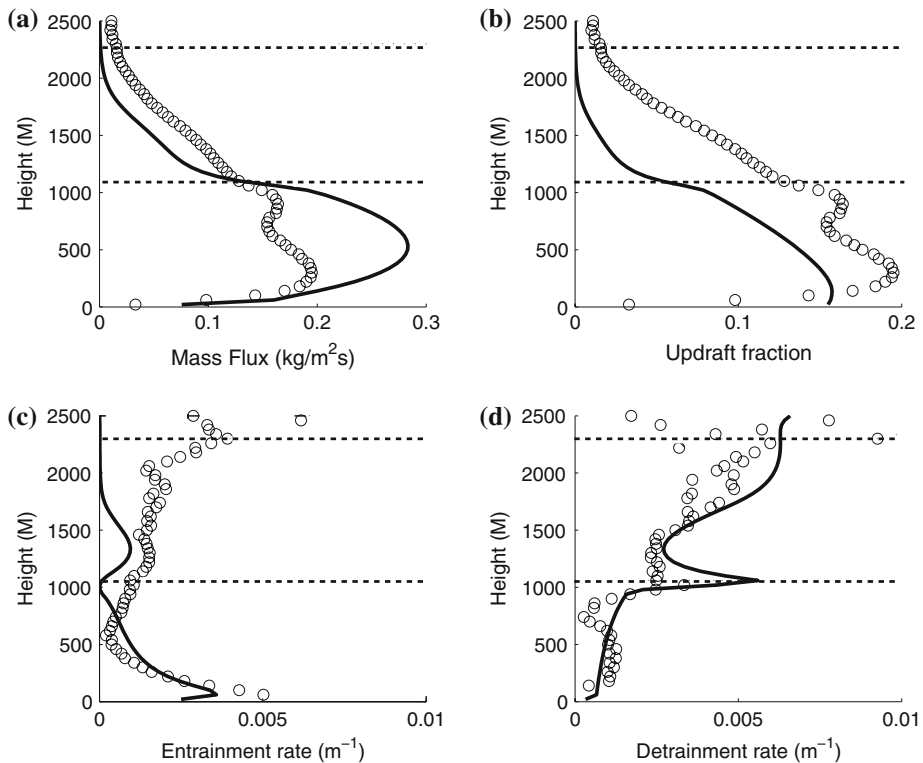
Fig. 9 ARM case: Mass flux (**a**), updraft fraction (**b**), entrainment ϵ (**c**) and detrainment δ (**d**) profiles after 8 h of simulation. *Solid line* represents 1D results and *circles* are LES values obtained by conditional sampling. The *dashed lines* represent the cloud base and top

To conclude, the scheme is able to diagnose clouds with depth, cloud fraction and liquid water mixing ratio in good agreement with LES results. In the 1D simulation, the mean cloud appears and dissipates approximately at the same moment as in LES and the mixing in the dry and cloudy portions of the CBL are well-represented compared to LES results. The new set of parameterizations was tested on another case of shallow cumulus convection obtained from a dataset collected during the Barbados Oceanographic and Meteorological Experiment (Holland and Rasmusson 1973). Similar results were found.

3.3.3 Updraft Variables

Several profiles representing updraft variables, such as the mass flux, the updraft fraction, the entrainment and detrainment rates, are shown in Fig. 9. For the SCM simulation, these variables were directly diagnosed from the convection scheme. For LES, a conditional sampling (CS in the following) based on the total water mixing ratio and the vertical velocity was used to determine the entrainment and detrainment rates in the subcloud and cloud layers. In short, this conditional sampling selects sufficiently moist and ascending grid points. Similarly to Berg and Stull (2002) a total water mixing ratio threshold is defined as a fraction of the standard deviation of its anomaly. Using a threshold proportional to the variance induces an automatic adaptation to the strength of turbulence. The CS is:

Point P $\in$ CS if $r_t > m \times min(\sigma_{rt}, \sigma_{min})$ and $w' > 0$ where

$$\sigma_{min}(z) = 0.05 \times \left(\frac{1}{z} \int\limits_{0}^{z} \sigma_{rt}(k)dk \right).$$

There is no threshold for the vertical velocity since the only constraint is that the parcel must be ascending. A minimum threshold is introduced. Its value of 5% of the average standard deviation at lower levels ensures that no point is selected in a non-turbulent environment where a standard deviation is still defined, as above the cloud layer. This CS was applied at each vertical level independently. Note that this CS compares well with the cloud and core sampling proposed by Siebesma and Cuijpers (1995) up to hour 9 of ARM. Afterwards, there is some difference due to the fact that this CS also selects air that is detrained out of the cloud. This induces a slight overestimation of the entrainment rate in the upper part of the cloud layer compared to cloud or core sampling. However, this sampling has the advantage of sampling the updraft continuously from the surface to the top of the CBL.

Entrainment and detrainment rates used in the parameterization are compared with those obtained by CS from LES in Fig. 9c and d. In the lower dry part, we note that the entrainment is well-represented with large values near the ground modelling the main source of air in the updraft coming from just above the ground. The minimum of entrainment is located near the inversion in the SCM results whereas, in LES, the minimum of entrainment is located in the middle of the CBL. The dry detrainment values are consistent with those obtained by LES notably near the inversion where the detrainment increase is well-represented qualitatively and quantitatively.

In the dry part, the mass flux shows good behaviour notably at the cloud base (Fig. 9a). This is explained by the continuous computation of mass flux from the sub-cloud layer to the cloud layer, which enables a reasonable representation of mass flux at cloud base. Concerning the updraft fraction, the 1D fraction is slightly smaller than that obtained from LES. In their intercomparison study, Brown et al. (2002) obtained a maximum updraft fraction of 10–15% at about 19h (UTC) (equivalent to 8 h of our simulation), which is consistent with our values. Moreover, in the dry part the order of magnitude of the updraft fraction, and also its vertical trend, are comparable to LES results.

In the cloudy part, SCM entrainment is weaker than in LES but both have the same order of magnitude. The SCM detrainment is consistent with LES. Figure 9a shows that the mass flux is underestimated but its vertical trend is consistent with LES mass flux obtained by CS. This is correlated with the weakness of the SCM entrainment and can explain the relative weakness of the turbulent fluxes in the cloudy part. But, as we have shown previously, the impact is weak on the mixing of θ_l and r_t and on the diagnosis of cloud characteristics. The SCM updraft fraction is too small but our updraft fraction represents the cloud core while the updraft fraction obtained by this CS corresponds more to the cloud fraction.

3.4 Stratocumulus-Topped Boundary Layer

3.4.1 Stratocumulus: Evolution and Impact of the New Scheme

It has been shown that the new parameterization satisfactorily represents cloud-free and cumulus CBL regimes. In some models, before running physical parameterizations, a diagnostic
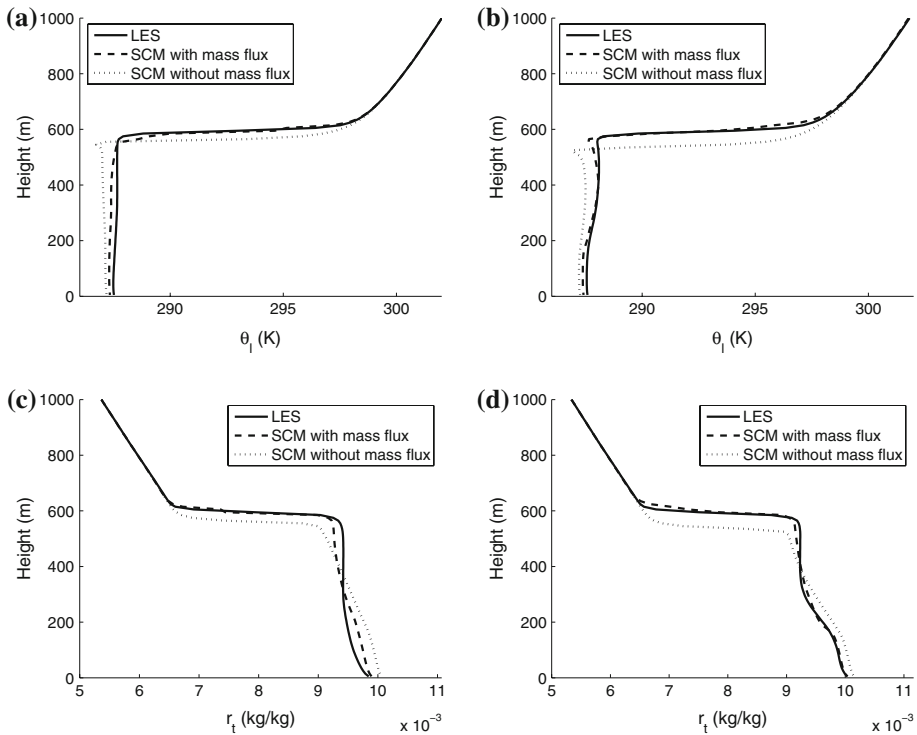
Fig. 10 FIRE case: Vertical profiles of liquid potential temperature θ_l at **a** 0600 and **b** 1200 local time and total mixing ratio r_t at **c** 0600 and **d** 1200 local time. *Solid line* shows LES results, *dashed line* the 1D profile with the new parameterization, and *dotted line* the profile obtained using only the turbulence scheme

of the PBL regime is performed in order to choose the parameterization consistent with this regime. For example, if the PBL is diagnosed as convective, the mass flux convective scheme is run to represent the impact of the thermals. But in the natural world, physical processes are continuous and there is no discontinuity between different PBL regimes. So, we chose to test our parameterization on a stratocumulus-topped boundary layer (STBL) case to show how the new scheme behaves in this type of regime. We expected that the contribution of the mass-flux term in the computation of the turbulent fluxes to be weak compared to the contribution of the eddy-diffusivity term.

In the case of stratocumulus, the mass flux must not lead to an over-strong mixing in the PBL, otherwise the stratocumulus clouds will disappear and a CBL will be created. This type of scheme is not suitable to an STBL but two points of our scheme encourage us to believe that the applicability of our parameterization to different regimes of PBL (notably the STBL) is possible. First, the closure of the scheme limits the strength of the mass flux if surface fluxes are weak. Second, having adaptive dry entrainment and detrainment depending on the type and the strength of the convection limits the impact of the scheme if conditions are not favourable for convection development.

The dynamics of stratocumulus is strongly influenced by top entrainment and radiative cooling at the cloud top. Without describing the dynamics of these clouds in detail, it should be noted that stratocumulus clouds are generally marked by a diurnal cycle (Wood et al. 2002); the evolution of the stratocumulus is closely related to radiative effects. During nighttime,
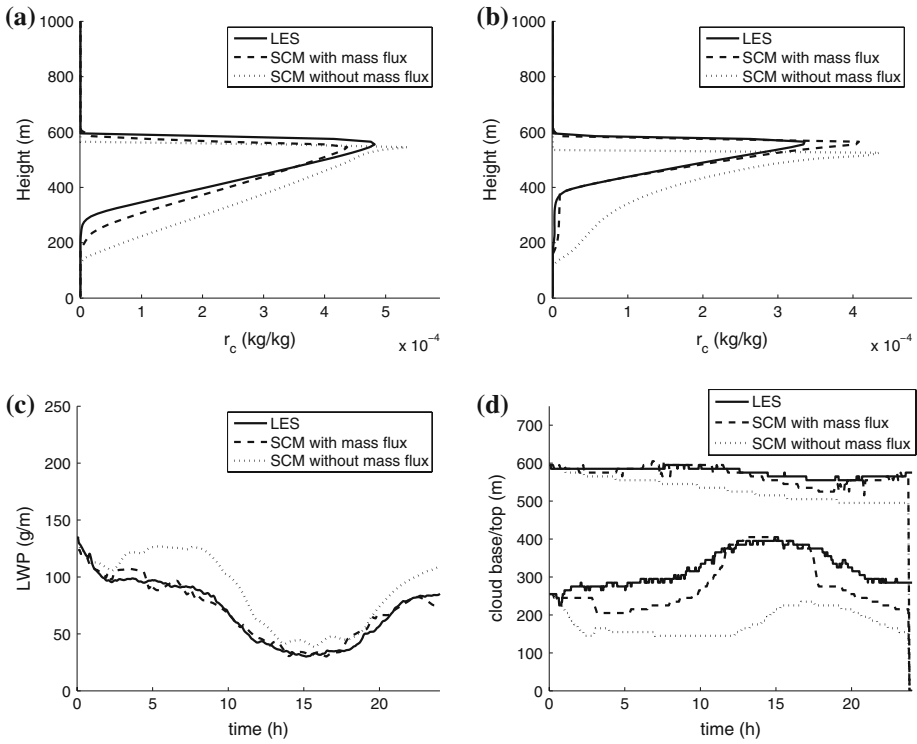
Fig. 11 FIRE case: Vertical profiles of liquid mixing ratio r_c at **a** 0600 and **b** 1200 local time. *Solid thin line* shows LES results, *dashed line* the 1D profile with the new parameterization, and *dotted line* the profile obtained using only the turbulence scheme; **c** and **d** the liquid water path (LWP) and heights of cloud base and top as a function of local time

the STBL is cooled at its top by radiative cooling due to emission of longwave radiation by the cloud and warmed and moistened at its base by the surface fluxes (Duynkerke et al. 1995). Thus, turbulence can be generated and is sufficient to mix the whole PBL. Profiles of conservative variables are well-mixed during the night. During daytime, stratocumulus are affected by the absorption of solar radiation, which can compensate for radiative cooling decreasing the turbulence intensity in the cloud. This can lead to a decoupling between the cloud layer and the subcloud layer by creating a stable layer under the cloud (Nicholls 1984).

Top entrainment is another important physical process in the evolution of the stratocumulus; it was studied by Lilly (1968) who developed a model of mixed layers. This process can accentuate the turbulence in the cloud and generate an elevation of the cloud base and a splitting up of the cloud, sometimes leading to its total dissipation. In Lilly (1968), Randall (1980) and Deardorff (1980a), entrainment is considered as a consequence of the local turbulent mixing. However, recent studies have shown that top-entrainment is caused by large-eddy turbulent motions scaled by the height of the PBL (Lewellen and Lewellen 1998, 2002).

3.4.2 The EUROCS\FIRE Case

The EUROCS\FIRE case study is a well-documented case of a STBL. LES and SCM simulations were initialized from observations collected in marine stratocumulus off the coast

of California in July 1987 during the First International Satellite Cloud Climatology Project (ISCCP) Regional Experiment (FIRE) (Hignett 1991; Duynkerke and Hignett 1995). This case is a part of the EUROCS project. Duynkerke et al. (2004) have realized both LES and SCM intercomparisons on this case. The same initialization, forcing, and vertical grid, as described in Duynkerke et al. (2004), were used here for the LES and SCM simulations. The sea surface temperature and surface pressure were prescribed as in Duynkerke et al. (2004) but contrary to the previous cases, fluxes were not prescribed but computed by the radiation scheme. The used microphysics scheme was a one-moment parameterization. Our simulations were limited to 24 h and not 48 h as in Duynkerke et al. (2004). Configurations of these simulations are summarized in Table 2. Note that the constants of the scheme used for the CBL cases are the same as described before; this reinforces the possible use of the scheme in NWP.

Figure 10 shows θ_l and r_t profiles at night (0600 local time) and during the day (1200 local time). The strength of the inversion is approximately 12 K. During nighttime, profiles obtained with the turbulence scheme only are not satisfactory: the inversion is too low, the profile of θ_l is unstable through the whole PBL, and the r_t profile is not mixed, the value being too high at the ground. With the new scheme, profiles are well mixed and values of θ_l and r_t are consistent with LES results. The inversion is well located. During daytime, the turbulence scheme also shows deficiencies. The simulated inversion is too low and θ_l too low. The decoupling is not really marked, and is particularly apparent on the r_t profile where the stable layer under the cloud is not well established. These failures are corrected by the contribution of the mass flux: θ_l and r_t values are consistent with the LES results, notably in the decoupling zone under the cloud.

The mass flux scheme improves the mixing in the cloud and subcloud layers. θ_l and r_t are well modelled compared to LES results and cause a better representation of the cloud characteristics. The representation of the liquid water path (LWP) and the liquid mixing ratio r_c is improved by the contribution of the mass flux term (Fig. 11). The fact that LWP values are consistent with LES results, enables a better modelling of the radiative fluxes in the cloud layer. The LES captures the diurnal evolution of the LWP due to solar radiation.

Duynkerke et al. (2004) have shown that the LWP is very sensitive to small changes in the thermodynamic structure of the STBL. A difference of 5% in the cloud thickness can imply a variation in the LWP of 20%. The new parameterization improves the evolution of cloud in terms of r_c, and cloud top and cloud base during daytime and nighttime (Fig. 11a, b, d) compared to the results obtained without the mass flux term. Using only the turbulence scheme does not enable the diurnal evolution of the cloud top to be simulated well: its height decreases constantly during the day (Fig. 11d). The cloud top obtained with the new scheme compares better with LES results.

We conclude that the turbulence scheme is not sufficient to represent top entrainment in stratocumulus. As described in the previous section, this process is crucial in the modelling of this type of cloud. Duynkerke et al. (2004) point out this general discrepancy of SCMs, and show the necessity of developing a top-entrainment parameterization for a better representation of stratocumulus.

Here, during nighttime, the mass flux term allows top entrainment of free atmosphere air into the PBL and improves the mixing over the whole STBL, as in the dry CBL. During daytime, the mass flux is limited to the subcloud layer due to the stable layer under the cloud and the top entrainment is weaker than at night. The mass flux contribution plays the role of top-entrainment parameterization and considerably improves the representation of the strato-cumulus diurnal evolution. As in the recent study by Lewellen and Lewellen (1998, 2002), the top entrainment in the STBL is mainly due to coherent structures and not to local turbulence.

4 Conclusion

In order to improve the mixing in the CBL, a mass flux part was incorporated into the computation of turbulent fluxes. This approach named EDMF for eddy diffusivity\mass flux, has been largely accepted by the community for parameterizing dry and shallow convection. The computation of turbulent fluxes is divided into two parts: the eddy-diffusivity term representing the local mixing and the mass flux term to represent the impact of the large eddies.

Results obtained with SCM have been compared to LES results. The global behaviour of the scheme has been tested on dry (IHOP) and cloudy diurnal convective cases (EUROCS\ARM) and also on an STBL case (EUROCS\FIRE).

This new set of parameterizations is able to correctly represent the mixing in the counter-gradient zone taking the effect of the non-local mixing (large eddies) into account in the upper part of the dry CBL. Compared to the results obtained using only the turbulence scheme, adding a mass flux term notably enabled the representation of fluxes opposed to the gradient of $\overline{\theta}_l$. Moreover, the mixing of momentum has been improved. The mass flux term is also responsible for overshooting, enabling better modelling of the top entrainment and leading to a better representation of the boundary-layer growth.

Results for EUROCS\ARM case have shown that the subgrid condensation, using the updraft variables, is able to correctly diagnose the cloud characteristics qualitatively and quantitatively. Cloud base and top are well located, and the liquid water content and the cloud fraction are in good agreement with those obtained using LES. We have also shown, using LES diagnostics, that entrainment and detrainment rates are well represented in the dry portion, even if entrainment is not strong enough in clouds.

Results for the \FIRE case have shown that the scheme is not only able to correctly represent the growth of the boundary layer from a nocturnal stable layer to a CBL but can also improve the dynamics of an STBL. The mass flux term is responsible for a better top entrainment leading to a better evolution of the LWP and better modelling of the decoupling during daytime compared to results obtained without a mass flux scheme. Moreover, the cloud top and base are consistent with LES results. Although, the cause of top entrainment is not explicitly known, taking the impact of coherent structures into account improves the modelling of the STBL.

Compared to other EDMF parameterizations, our approach contains several important improvements enabling these three types of boundary-layer regime to be well represented:

- *new closure for the mass flux* at the ground solves the closure problem at the LCL studied by Neggers et al. (2004).
- computing *adaptative dry entrainment and detrainment from updraft buoyancy and vertical velocity* enables representation of the evolution of the CBL and also the STBL to be represented without differentiating the type of PBL regime.
- *Kain–Fritsch approach* enables variations of entrainment and detrainment in cumulus.
- the *new subgrid condensation scheme* improves the representation of the cloud characteristics notably for the cloud fraction.
- *one updraft* is used to keep real continuity between the subcloud layer and the cloud layer.

This robustness of the scheme for different PBL regimes allows it to be included in NWP models.

Appendix

1 Mass Flux in the Surface Layer Compared to w_*

The mass flux near the surface was set proportional to the convective vertical velocity scale w_* as in Grant (2001). The coefficient of proportionality C_{M_0} in our scheme cannot have the same value as that used by Grant (2001) due to the fact that Grant (2001) defines this relation at the LCL. So, we used the conditional sampling defined in Sect. 3.3.3 to obtain mass flux values in the surface layer for different convective cases at different dates (IHOP, ARM).

Figure 12 is a plot of the surface layer mass flux against sub-cloud layer velocity scale. The LES data suggest that $C_{M_0} = 0.065$.

2 Analytical Solution for the Vertical Velocity w_u

Equation 7 presents the computation for vertical velocity in the updraft w_u. Combining with the equation for entrainment 14, the w_u equation becomes:

$$\frac{\partial w_u^2}{\partial z} = 2aB_u - 2bC_\epsilon max(0, B_u) \tag{20}$$

Fig. 12 Mass flux in the surface layer computed using the conditional sampling defined in Sect. 3.3.3 versus sub-cloud layer velocity scale w_*. *Line* shows $M = 0.065w_*$

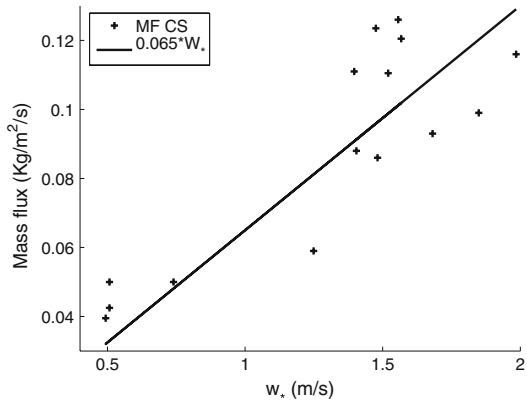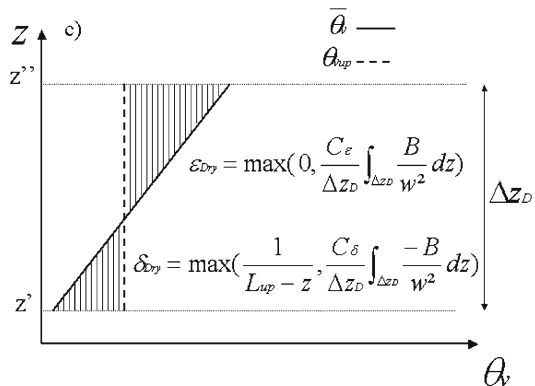**Fig. 13** Parameterized entrainment and detrainment for the dry layer

C_{BUO} is defined equal to $2a$ if $B_u < 0$ (entrainment is zero) and to $2(a - bC_\epsilon)$ if $B_u > 0$. This equation is integrated over each layer. Figure 13 presents this integral. If z' is layer bottom, z'' is layer top and $\Delta z_D = z'' - z'$, $w_u{}^2$ is defined by:

$$\int_{\Delta z_D} \frac{\partial w_u{}^2}{\partial z} dz = \int_{\Delta z_D} C_{BUO} B_u dz, \tag{21}$$

$$w_u{}^2(z'') - w_u{}^2(z') = C_{BUO} \frac{g}{\theta_{ref}} \int_{\Delta z_D} \left[\theta_{v_{up}}(z) - \overline{\theta_v}(z) \right] dz, \tag{22}$$

where $\theta_{v_{up}}$ is assumed constant between z' and z'', and the variations of $\overline{\theta_v}$ is assumed to be linear between z' and z''.

$$\overline{\theta_v}(z) = \alpha_1 z + \overline{\theta_v}(z'), \tag{23}$$

$$\theta_{v_{up}}(z) = \theta_{v_{up}}(z'). \tag{24}$$

So, the integral for w_u becomes

$$w_u{}^2(z'') - w_u{}^2(z') = C_{BUO} \frac{g}{\theta_{ref}} \int_{\Delta z_D} \left[-\alpha_1 z - \overline{\theta_v}(z') + \theta_{v_{up}}(z') \right] dz. \tag{25}$$

After computation, w_u at the level z'' computed from the level z' is:

$$w_u{}^2(z'') = C_{BUO} \frac{g}{\theta_{ref}} \Delta z_D \left(\frac{-\alpha_1}{2} \Delta z_D - \overline{\theta_v}(z') + \theta_{v_{up}}(z') \right) + w_u{}^2(z'). \tag{26}$$

3 Analytical Integrated Solution for Entrainment and Detrainment

The entrainment ϵ is defined by the Eq. 14. This equation is integrated, like w_u, on each vertical grid size, for example between z' and z'' (see Fig. 13):

$$\epsilon = \frac{C_\epsilon}{\Delta z_D} \int_{\Delta z_D} \frac{B}{w_u{}^2} dz. \tag{27}$$

Using Eq. 26, ϵ becomes

$$\epsilon = \frac{C_\epsilon g}{\Delta z_D \theta_{ref}} \int_{\Delta z_D} \frac{\theta_{v_{up}}(z') - \alpha_1 z + \overline{\theta_v}(z')}{C_{BUO} \frac{g}{\theta_{ref}} z(-\alpha_1 z - \overline{\theta_v}(z') + \theta_{v_{up}}(z')) + w_u{}^2(z')} dz, \tag{28}$$

$$\epsilon = \frac{C_\epsilon}{\Delta z_D C_{BUO}} \int_{\Delta z_D} \frac{-\alpha_1 z + \theta_{v_{up}}(z') + \overline{\theta_v}(z')}{\frac{-\alpha_1}{2} z^2 - \overline{\theta_v}(z')z + \theta_{v_{up}}(z')z + \frac{\theta_{ref} w_u{}^2(z')}{g C_{BUO}}} dz, \tag{29}$$

noting that $X = \frac{-\alpha_1}{2} z^2 - \overline{\theta_v}(z')z + \theta_{v_{up}}(z')z + \frac{\theta_{ref} w_u{}^2(z')}{g C_{BUO}}$:

$$dX = ((-\alpha_1)z + \theta_{v_{up}}(z') + \overline{\theta_v}(z'))dz, \tag{30}$$

$$\epsilon = \frac{C_\epsilon}{C_{BUO} \Delta z_D} \int_{\Delta z_D} \frac{dX}{X}, \tag{31}$$

$$\epsilon = \frac{C_\epsilon}{C_{BUO} \Delta z_D} [Ln(X)]_{\Delta z_D}. \tag{32}$$

After computation, ϵ is defined as:

$$\epsilon = \frac{C_\epsilon}{C_{BUO} \Delta z_D} ln \left[1 + \frac{C_{BUO} \Delta z_D}{w_u{}^2(z') \theta_{ref}} (\frac{-\alpha_1}{2} \Delta z - \theta_{v_{up}}(z') + \overline{\theta_v}(z')) \right] \tag{33}$$

where α_1 is defined as previously. An identical solution can be found for δ taking the absolute value of the buoyancy.

A formulation of the transition between cloudy and dry regime is added to limit the sensitivity of the scheme to the change in the computation of entrainment and detrainment. If a liquid mixing ratio is detected at z'' using an "all or nothing" adjustment from updraft variables, the LCL height is determined assuming a linear increase of r_c with height. A weight for the KF90 lateral exchanges is defined as proportional to the cloudy part occupation of the grid and the integral dry entrainment and detrainment are computed only on the height of the dry part.

References

Arakawa A (2004) The cumulus parameterization problem: past present and future. J Clim 17:2493–2525

Arakawa A, Schubert WH (1974) Interaction of a cumulus cloud ensemble with the large-scale environment, Part 1. J Atmos Sci 31:674–700

Bechtold P, Cuijpers JWM (1995) Cloud perturbations of temperature and humidity: a LES study. Boundary-Layer Meteorol 76:377–386

Bechtold P, Bazile E, Guichard F, Mascart P, Richard E (2001) A mass-flux convection scheme for regional and global models. Q J Roy Meteorol Soc 127:869–886

Berg LK, Stull RB (2002) Accuracy of point and line measures of boundary layer cloud amount. J Appl Meteorol 41:640–650

Betts AK (1973) Nonprecipitatting cumulus convection and its parameterization. Q J Roy Meteorol Soc 99:178–196

Bougeault P, Lacarrère P (1989) Parameterization of orography-induced turbulence in a mesobeta-scale model. Mon Weather Rev 117:1872–1890

Brown A, Cederwall RT, Chlond A, Duynkerke PG, Golaz JC, Khairoutdinov M, Lewellen D, Lock AP, Macvean MK, Moeng CH, Neggers RAJ, Siebesma P, Stevens B (2002) Large-eddy simulation of the diurnal cycle of shallow cumulus convection over land. Q J Roy Meteorol Soc 128:1075–1093

Browning KA (1993) The GEWEX Cloud System Study (GCSS). Bull Am Meteorol Soc 74:387–399

Buckingham E (1914) On physically similar systems: illustrations of the use of dimensional equations. Phys Rev IV:345–376

Cheinet S (2003) A multiple mass-flux parameterization for the surface-generated convection, Part 1: dry plumes. J Atmos Sci 60:2313–2327

Clarke RH, Dyer AJ, Reid DG, Troup AJ (1971) The Wangara experiment: boundarylayer data. Division Meteorological Physics Paper No. 19: CSIRO, Australia

Couvreux F, Guichard F, Redelsperger JL, Kiemle C, Masson V, Lafore JP, Flamant C (2005) Water–vapour variablility within a convective boundary-layer assessed by large-eddy simulations and IHOP2002 observations. Q J Roy Meteorol Soc 131:2665–2693

Cuijpers JWM, Holtslag AM (1998) Impact of skewness and nonlocal effects on scalar and buoyancy fluxes in convective boundary layers. J Atmos Sci 55:151–162

Cuxart J, Bougeault P, Redelsperger JL (2000) A turbulence scheme allowing for mesoscale and large-eddy simulations. Q J Roy Meteorol Soc 126:1–30

De Roode SR, Duynkerke PG, Siebesma P (2000) Analogies between mass-flux and Reynolds-averaged equations. J Atmos Sci 57:1585–1598

De Rooy WC, Siebesma P (2008) A simple parameterization for detrainment in shallow cumulus. Mon Weather Rev 136:560–576

Deardorff JW (1966) The counter-gradient heat flux in the lower atmosphere and in the laboratory. J Atmos Sci 23:503–506

Deardorff JW (1980a) Cloud top entrainment instability. J Atmos Sci 37:131–147

Deardorff JW (1980b) Stratocumulus-capped mixed layers derived from a three-dimensionnal model. Boundary-Layer Meteorol 18:495–527

Duynkerke PG, Hignett P (1995) Simulation of diurnal variation in a stratocumulus-capped marine boundary layer during FIRE. Mon Weather Rev 52:2763–2777

Duynkerke PG, Zhang H, Jonker PJ (1995) Microphysical and turbulent structure of nocturnal stratocumulus as observed during astex. J Atmos Sci 52:2763–2777

Duynkerke PG, De Roode SR, Van Zanten MC, Calvo J, Cuxart J, Cheinet S, Chlond A, Grenier H, Jonker PJ, Kohler M, Lenderink G, Lewellen D, Lappen CL, Lock AP, Moeng CH, Muller F, Olmeda D, Piriou JM,

Sanchez E, Sednev I (2004) Observations and numerical simulations of the diurnal cycle of the EUROCS stratocumulus case. Q J Roy Meteorol Soc 130:3269–3296

Grant ALM (2001) Cloud-base fluxes in the cumulus-capped boundary layer. Q J Roy Meteorol Soc 127:407–421

Gregory D, Kershaw R, Inness PM (1997) Parametrization of momentum transport by convection. II: tests in single-column and general circulation models. Q J Roy Meteorol Soc 123:1153–1183

Hignett P (1991) Observations of the diurnal variation in the cloud-capped marine boundary layer. J Atmos Sci 45:1474–1482

Holland JZ, Rasmusson EM (1973) Measurement of atmospheric mass, energy and Momentum budgets over a 500-kilometer square of tropical ocean. Mon Weather Rev 101:44–55

Holtslag AAM, Moeng CH (1991) Eddy diffusivity and countergradient transport in the convective atmospheric boundary layer. J Atmos Sci 48:1690–1698

Hourdin F, Couvreux F, Menut L (2002) Parameterization of the dry convective boundary layer based on a mass flux representation of thermals. J Atmos Sci 59:1105–1122

Kain JS, Fritsch JM (1990) A one-dimensionnal entraining/detraining plume model and its application in convective parameterization. J Atmos Sci 47:2784–2802

Lafore JP, Stein J, Asencio N, Bougeault P, Ducrocq V, Duron J, Fisher C, Hereil P, Mascart P, Masson V, Pinty JP, Redelsperger JL, Richard E, Arellano JV (1998) The meso-NH atmospheric simulation system, Part I: adiabatic formulation and control simulations. Ann Geophys 16:90–109

Lappen CL, Randall DA (2001) Toward a unified parameterization of the boundary layer and moist convection, Part 2: lateral mass exchanges and subplume-scale fluxes. J Atmos Sci 58:2037–2051

Lenderink G, Siebesma P, Cheinet S, Irons S, Jones CG, Marquet P, Muller F, Olmeda D, Calvo J, Sanchez E, Soares PMM (2004) The diurnal cycle of shallow cumulus clouds over land: a single column model intercomparaison study. Q J Roy Meteorol Soc 130:3339–3364

Lewellen D, Lewellen W (1998) Large-eddy boundary layer entrainment. J Atmos Sci 55:2645–2665

Lewellen D, Lewellen W (2002) Entrainment and decoupling relations for cloudy boundary layers. J Atmos Sci 59:2966–2987

Lilly DK (1968) Models of cloud-topped mixed layers under a strong inversion. Q J Roy Meteorol Soc 94:292–309

Neggers RAJ, Siebesma P, Jonker HJJ (2002) A multiparcel model for shallow cumulus convection. J Atmos Sci 59:1655–1668

Neggers RAJ, Siebesma AP, Lenderink G, Holtslag AM (2004) An evaluation of mass flux closures for diurnal cycles of shallow cumulus. Mon Weather Rev 132:2525–2538

Nicholls S (1984) The dynamics of stratocumulus: aircraft observations and comparisons with a mixed layer model. Q J Roy Meteorol Soc 110:783–820

Ooyama K (1971) A theory on parameterization of cumulus convection. J Meteorol Soc Jpn 49:744–756

Randall DA (1980) Conditionnal instability of the first kind upside-down. J Atmos Sci 37:125–130

Rio C, Hourdin F (2008) A thermal plume model for the convective boundary layer. J Atmos Sci 65:407–425

Schumann U (1987) The countergradient heat flux in stratified turbulent flows. Nucl Eng Des 100:255–262

Siebesma P (1998) Shallow cumulus convection. In: Plate EJ et al (eds) Buoyant convection in geophysical flows. Kluwer, Amsterdam, pp 441–486

Siebesma P, Cuijpers JWM (1995) Evaluation of parametric assumptions for shallow cumulus convection. J Atmos Sci 53:650–666

Siebesma P, Holtslag AM (1996) Model impacts of entrainment and detrainment rates in shallow cumulus convection. J Atmos Sci 53:2354–2364

Siebesma P, Teixeira J (2000) An advection-diffusion scheme for the convective boundary layer, description and 1D results. In: Proceedings of 14th symposium on boundary layers and turbulence, Aspen, USA, pp 133–136

Siebesma P, Bretherton CS, Brown A, Chlond A, Cuxart J, Duynkerke PG, Jiang H, Khairoutdinov M, Lewellen D, Moeng CH, Sanchez E, Stevens B, Stevens DE (2003) A large eddy simulation intercomparison study of shallow cumulus convection. J Atmos Sci 60:1201–1219

Siebesma P, Soares PMM, Teixeira J (2007) A combined eddy-diffusivity mass-flux approach for the convective boundary layer. J Atmos Sci 64:1230–1248

Simpson J, Wiggert V (1969) Models of precipitating cumulus towers. Mon Weather Rev 97:471–489

Soares PMM, Miranda PMA, Siebesma AP, Teixeira J (2004) An eddy-diffusivity/mass-flux parameterization for dry and shallow cumulus convection. Q J Roy Meteorol Soc 130:3055–3079

Stull RB (1988) An introduction to boundary layer meteorology. Kluwer, Dordrecht, 666 pp

Sullivan PP, Moeng CH, Stevens B, Lenschow DH, Mayor SD (1998) Structure of the entrainment zone capping the convective. J Atmos Sci 55:3042–3064

Taylor GR, Baker MB (1991) Entrainment and detrainment in cumulus clouds. J Atmos Sci 48:112–121

Teixeira J, Stevens B, Bretherton CS, Cederwall R, Doyle JD, Golaz JC, Holtslag AMM, Klein SA, Lundquist JK, Randall DA, Siebesma AP, Soares PMM (2008) Parameterization of the atmospheric boundary layer: a view from just above the inversion. Bull Am Meteorol Soc 89:453–458

Tiedtke M (1989) A comprehensive mass-flux scheme for cumulus parameterization in large-scale models. Mon Weather Rev 177:1779–1800

Tomas S, Masson V (2006) A parametrization of third order moments for dry convective boundary layer. Boundary-Layer Meteorol 120:437–454

Troen IB, Mahrt L (1986) A simple model of the atmospheric boundary layer: sensitivity to surface evaporation. Boundary-Layer Meteorol 37:129–148

Wang S, Stevens B (2000) Top-hat representation of turbulence statistics in cloud-topped boundary layers: a large eddy simulation study. J Atmos Sci 57:423–441

Weckwerth TM, Parsons DB, Koch SE, Moore JA, Lemone MA, Demoz BR, Flamant C, Geerts B, Wang J, Feltz W (2004) An overview of the international H2O project (IHOP_2002) and some preliminary highlights. Bull Am Meteorol Soc 85:253–277

Wood R, Bretherton CS, Hartmann DL (2002) Diurnal cycle of liquid water path over the subtropical and tropical oceans. Geophys Res Lett 29:7.1–7.4

Yanai M, Esbensen S, Chu J (1973) Determination of bulk properties of tropical cloud clusters from large-scale heat and moisture budgets. J Atmos Sci 30:611–627

Young GS (1988) Turbulence structure of the convective boundary layer, Part II: Phoenix 78 Aircraft observations of thermals and their environment. J Atmos Sci 45:727–735

Zhao M, Austin PH (2003) Episodic mixing and buoyancy-sorting representations of shallow convection: a diagnostic study. J Atmos Sci 60:892–912